Nonadiabatic molecular dynamics simulation of $C_2H_2^{2+}$ in a strong laser field

Ji-Gen Chen(陈基根), Gang-Tai Zhang(张刚台), Ting-Ting Bai(白婷婷), Jun Wang(王俊), Ping-Ping Chen(陈平平), Wei-Wei Yu(于伟威), Xi Zhao(赵曦)

Citation: Chin. Phys. B . 2020, 29(11): 113202 . **doi:** 10.1088/1674-1056/abb3de
Journal homepage: http://cpb.iphy.ac.cn; http://iopscience.iop.org/cpb

What follows is a list of articles you may be interested in

Resonance-enhanced two-photon ionization of hydrogen atom in intense laser field investigated by Bohmian-mechanics

Yang Song(宋阳), Shu Han(韩姝), Yu-Jun Yang(杨玉军), Fu-Ming Guo(郭福明), Su-Yu Li(李苏宇)

Chin. Phys. B . 2020, 29(9): 093204 . **doi:** 10.1088/1674-1056/aba09e

Relative phase-dependent two-electron emission dynamics with two-color circularly polarized laser fields

Tong-Tong Xu(徐彤彤), Lian-Lian Zhang(张莲莲), Zhao Jin(金钊), Wei-Jiang Gong(公卫江)

Chin. Phys. B . 2020, 29(9): 093202 . **doi:** 10.1088/1674-1056/ab928c

Photoelectron imaging on vibrational excitation and Rydberg intermediate states in multi-photon ionization process of NH_3 molecule

Ya-Nan Sun(孙亚楠), Yan-Hui Wang(王艳辉), Le-Le Song(宋乐乐), Hai-Bin Du(杜海滨), Xiao-Chun Wang(王晓春), Lan-Lai He(赫兰海), Si-Zuo Luo(罗嗣佐), Qin Yang(杨钦), Jing Leng(冷静), Fu-Chun Liu(刘福春)

Chin. Phys. B . 2020, 29(9): 093201 . **doi:** 10.1088/1674-1056/ab9431

Role of potential on high-order harmonic generation from atoms irradiated by bichromatic counter-rotating circularly polarized laser fields

Xu-Xu Shen(申许许), Jun Wang(王俊), Fu-Ming Guo(郭福明), Ji-Gen Chen(陈基根), Yun-Jun Yang(杨玉军)

Chin. Phys. B . 2020, 29(8): 083201 . **doi:** 10.1088/1674-1056/ab961c

Validity of extracting photoionization time delay from the first moment of streaking spectrogram

Chang-Li Wei(魏长立), Xi Zhao(赵曦)

Chin. Phys. B . 2019, 28(1): 013201 . **doi:** 10.1088/1674-1056/28/1/013201

Nonadiabatic molecular dynamics simulation of $C_2H_2^{2+}$ in a strong laser field*

Ji-Gen Chen(陈基根)[1], Gang-Tai Zhang(张刚台)[2], Ting-Ting Bai(白婷婷)[3], Jun Wang(王俊)[4,†], Ping-Ping Chen(陈平平)[5,‡], Wei-Wei Yu(于伟威)[6,§], and Xi Zhao(赵曦)[7,8,9,¶]

[1] *Zhejiang Provincial Key Laboratory for Cutting Tools, Taizhou University, Taizhou* 225300, *China*
[2] *College of Physics and Optoelectronics Technology, Baoji University of Arts and Sciences, Baoji* 721016, *China*
[3] *College of Mathematics and Information Science, Baoji University of Arts and Sciences, Baoji 721013, China*
[4] *Institute of Atomic and Molecular Physics, Jilin University, Changchun* 130012, *China*
[5] *Industrial and Manufacturing Systems Engineering, Kansas State University, Manhattan, KS* 66506, *USA*
[6] *School of Physics and Electronic Technology, Liaoning Normal University, Dalian* 116029, *China*
[7] *School of Physics and Information Technology, Shaanxi Normal University, Xi'an* 710062, *China*
[8] *School of Physics and Electronics, Qiannan Normal College For Nationalities, Guizhou Province, Duyun* 558000, *China*
[9] *Department of Physics, Kansas State University, Manhattan, KS* 66506, *USA*

(Received 19 February 2020; revised manuscript received 19 August 2020; accepted manuscript online 1 September 2020)

We investigate the alignment dependence of the strong laser dissociation dynamics of molecule $C_2H_2^{2+}$ in the frame of real-time and real-space time-dependent density function theory coupled with nonadiabatic quantum molecular dynamics (TDDFT-MD) simulation. This work is based on a recent experiment study "ultrafast electron diffraction imaging of bond breaking in di-ionized acetylene" [Wolter *et al*, *Science* **354**, 308–312 (2016)]. Our simulations are in excellent agreement with the experimental data and the analysis confirms that the alignment dependence of the proton dissociation dynamics comes from the electron response of the driving laser pulse. Our results validate the ability of the TDDFT-MD method to reveal the underlying mechanism of experimentally observed and control molecular dissociation dynamics.

Keywords: strong field physics, molecular dynamics, TDDFT, attosecond science, ultra fast optics

PACS: 32.80.Rm, 42.50.Hz, 42.65.Ky **DOI:** 10.1088/1674-1056/abb3de

1. Introduction

Recent advances in the production of extremely ultra-intense laser pulse techniques have stimulated an increasing interest in the main problem of laser and matter interaction.[1–17] Especially, complete control of molecular dynamic and reaction is one of the central aims of photophysical and photochemical science. Recent progress in laser technology has made time-domain observation of reaction dynamics available. In 2016, one study showed that the strong laser fields can effectively manipulate the proton dissociation molecular dynamics.[1] In Ref. [1], the authors combined mid-infrared (mid-IR) laser-induced electron diffraction (LIED) with single molecule C_2H_2 coincidence detection in a reaction microscope and used an additional laser control field to impulsively align the molecule:[1] first, a 1700-nm controlled laser pulse used to orient the C_2H_2 molecule parallel or perpendicular to the LIED field; then a 3100-nm LIED laser field triggers the molecular ionization, dissociation, and images the structural snapshots of C_2H_2 molecule.[1] In a theoretical simulation point of view, the three processes of orientation, ionization, and dissociation can be carried out independently. Furthermore, the mechanisms of orientation and ionization are well explained in Ref. [1], the authors in Ref. [1] gave a briefly theoretical explanation and their simulation results matched well with the experimental data. However, the role of the electron response in the proton dissociation dynamic is still unclear. Therefore, the objective of this paper is to understand the effect of the electron response on the strong laser proton dissociation dynamic. As we know, strong laser pulses may cause fast molecular structural rearrangement during the interaction between the laser pulse and the molecule, thus, adiabatic molecular dynamics model

*Xi Zhao was supported by Chemical Sciences, Geosciences, and Biosciences Division, Office of Basic Energy Sciences, Office of Science, U.S. Department of Energy (Grant No. DE-FG02-86ER13491), the National Natural Science Foundation of China (Grant No. 11904192); Ji-Gen Chen was supported by the National Natural Science Foundation of China (Grant No. 11975012); Gang-Tai Zhang was supported by the Natural Science Basic Research Plan of Shaanxi Province, China (Grant No. 2016JM1012), the Natural Science Foundation of the Educational Department of Shaanxi Province, China (Grant No. 18JK0050), the Science Foundation of Baoji University of Arts and Sciences of China (Grant No. ZK16069); Jun Wang was supported by the National Natural Science Foundation of China (Grant Nos. 11604119 and 11627807); and Wei-Wei Yu was supported by the National Natural Science Foundation of China (Grant No. 11604131).

†Corresponding author. E-mail: wangjun86@jlu.edu.cn
‡Corresponding author. E-mail: pingpingchen@ksu.edu
§Corresponding author. E-mail: weiweiyu2012@163.com
¶Corresponding author. E-mail: zhaoxi719@ksu.com

is no more valid in this case. Therefore, it is necessary to take into account nonadiabatic molecular dynamics (NAMD) scheme. The TDDFT-MD simulation is a promising method in this respect.[18] To date, TDDFT have been employed to deal with a lot of highly nonlinear phenomena, such as multiphoton ionization,[19] high harmonic generation (HHG) in gases and solids,[20,21] as well as nonadiabatic molecular dynamics simulations.[18] Comparing with the other NAMD methods, such as Tully surface hopping,[22] multi configuration time-dependent Hartree (MCTDHF),[23] directly solving TDSE,[24] TDDFT-MD scheme has several advantages: it has favorable system-size scaling, and its efficiency allows calculations on large systems for even picoseconds; besides, TDDFT provides an efficient way to describe the strong laser field assisting electron response (ionization, excitation), which is the key part in this work. This is the reason why we choose TDDFT-MD method in this work.

In this paper, the potential energy curve, laser-assisted ionization, and dissociation dynamics is studied using DFT, TDDFT, and TDDFT-MD methods, respectively. Our results reveal that, the dynamics of one of the C–H band from parallel and perpendicular orientations are totally different. Meanwhile, another C–H band in parallel and perpendicular cases undergoes a similar dynamics. Our calculation and analysis show this difference comes from the ionization yield in parallel orientation is larger than perpendicular orientation. Therefore, the proton dynamics in parallel and perpendicular orientations are different. Our results validate the ability of the TDDFT-MD method to reveal the underlying mechanism of experimentally molecular dissociation dynamics.

The remainder of this paper is organized as follows. In Section 2, the TDDFT-MD method used to simulate the laser reaction dynamics are described. In Section 3, the proton dissociation dynamics, alignment-dependent electron ionization associating with the classical particle force analysis are given. Finally, a summary is given in Section 4. Atomic units (a.u.) are used throughout this article unless mentioned.

2. Theory and methods

In the present simulation, the DFT, TDDFT, and TDDFT-MD calculations were all performed using the OCTOPUS code.[25–27] In the frame of TDDFT, all the physical processes can be retrieved from the time-dependent electron density

$$\rho(r,t)=\sum_{\sigma}\sum_{i=1}^{N_\sigma}|\psi_{i\sigma}(r,t)|^2, \tag{1}$$

where σ, i, and N_σ are spin index, orbital index, and the number of electrons with spin σ, respectively. $\psi_{i\sigma}(r,t)$ is the time-dependent Kohn–Shan orbital, which satisfies the time-dependent Kohn–Shan equation

$$\mathrm{i}\frac{\partial\psi_{i\sigma}(r,t)}{\partial t}=\left[-\frac{1}{2}\nabla^2+V_{\mathrm{N-e}}(r)+V_{\mathrm{H}}(r,t)+V_{\mathrm{xc}}(r,t)+V_{\mathrm{ext}}(r,t)\right]\psi_{i\sigma}(r,t), \tag{2}$$

where $V_{\mathrm{N-e}}(r)$ is the nucleus–electron potential of the Coulomb interaction between electron and nuclei, we employ the form given by Troullier and Martins centered at each ion.[28] $V_{\mathrm{H}}(r,t)$ is Hartree potential of electron–electron Coulomb interaction. $V_{\mathrm{xc}}(r,t)$ is the exchange–correlation potential, In this article, this functional was approximated using the adiabatic local-density approximation (ALDA) with the parametrization of Perdew and Zunger.[29] $\varepsilon_{\mathrm{xc}}$ is the exchange–correlation energy density with functional dependence on the density $\rho(r,t)$. $V_{\mathrm{ext}}(r,t)$ describes the interaction between the molecule and the laser field. Using the dipole approximation it is expressed as

$$V_{\mathrm{ext}}(r,t)=f(t)\cos(\omega t)\,\hat{\varepsilon}\cdot r, \tag{3}$$

where $f(t)$, ω, and $\hat{\varepsilon}$ denote the temporal profile, the carrier frequency, and the polarization direction, respectively.

We describe the ion dynamics by Ehrenfest method where the forces acting on ions are evaluated from the electron-density distribution at each time step:

$$M_a\frac{\mathrm{d}^2}{\mathrm{d}t^2}R_a(t)=F_a^{\mathrm{e-i}}+F_a^{\mathrm{i-i}}+F_a^{\mathrm{ext-i}}, \tag{4}$$

where

$$F_a^{\mathrm{e-i}}=-\int\frac{\partial V_{\mathrm{N-e}}}{\partial R_a}\rho(r,t)\,\mathrm{d}r, \tag{5}$$

$$F_a^{\mathrm{i-i}}=\sum_b\frac{Z_aZ_b(R_b-R_a)}{|R_b-R_a|^3}, \tag{6}$$

$$F_a^{\mathrm{ext-i}}=Z_aE(t), \tag{7}$$

where Z_a and M_a are the electric charge and mass of ion a. The computational results presented in the next section use the following parameters. The spherical box is given with a radius 10. The molecular axis lies in the x direction. The grid spacing is 0.2. The time step for the propagation of the wave function is $\mathrm{d}t=0.01$. The parameters have been tested carefully.

3. Results and discussion

Because the laser intensity is strong and the molecular structure is complex, there should be several ionization pathways contributing to the C–H dissociation. These pathways can be distinguished from potential energy curve (PEC) calculation. Figure 1 is the PEC along C–H direction of C_2H_2, $C_2H_2^{1+}$ and $C_2H_2^{2+}$, respectively. There are

two main ionization–dissociation pathways contribution to $C_2H_2 \rightarrow C_2H_2^{2+} \rightarrow H^+ + C_2H^+$:[1,30] (i) the first one electron ionizes from σ_g-type highest occupied molecular orbital (HOMO)-1 of the ground state ($1\sigma_g^2 1\sigma_u^2 2\sigma_g^2 2\sigma_u^2 3\sigma_g^2 1\pi_u^2 1\pi_u^2$). Then the second electron ionizes from the π_u-type HOMO of the excited state $^2\Sigma_g^+$ of $C_2H_2^{1+}$, finally the molecule reaches first dissociative excited singlet and triplet states $^1\Pi_u$ and $^3\Pi_u$. (ii) The first electron tunnels from the HOMO of the neutral ground state $^1\Sigma_g^+$ to the singly ionic doublet $^2\Pi_u$ state, then the second electron tunnels from the HOMO of the singly ionic ground state to one of $C_2H_2^{2+}$ $^3\Sigma_g^-$, $^1\Delta_g$, and $^1\Sigma_g^+$ states. For the lifetimes of $C_2H_2^{2+}$ $^3\Sigma_g^-$, $^1\Delta_g$, and $^1\Sigma_g^+$ states are nanosecond level ($^3\Sigma_g^-$ lifetime is 108 nanoseconds[1]), thus, we are only interested in the direct dissociate channel leading to proton loss, that is, the (i) pathway.

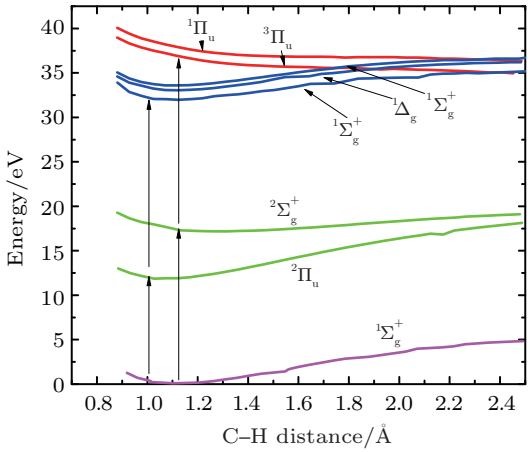

Fig. 1. The calculated relevant energy levels and two possible ionization–dissociation pathways. The lowest line is the ground state of neutral ground state $^1\Sigma_g^+$. The two green lines are the ground and excited states $^2\Pi_u$, $^2\Sigma_g^+$ of $C_2H_2^{1+}$. The upper six lines are the states of $C_2H_2^{2+}$.

According to our analysis above, we set the initial state of $C_2H_2^{2+}$ molecule to be $^3\Pi_u$ before the time propagating. The all-electron density distribution of the molecule is shown in Fig 2, as we can see, the electron density distributes most along the molecular axes.

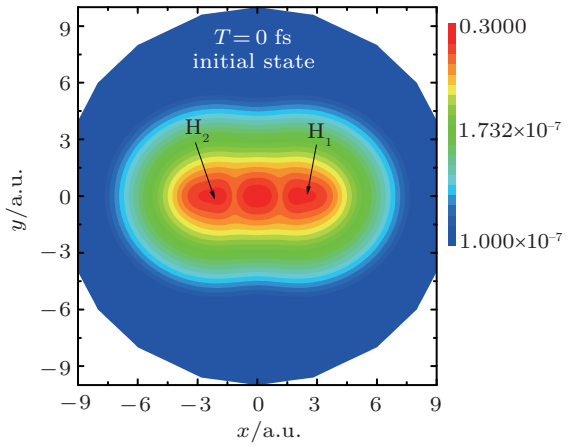

Fig. 2. Schematic geometry and initial electron density distribution of the $C_2H_2^{2+}$ molecule.

Firstly, we present our main results in Fig. 4, the time evolution of different chemical bonds at parallel and perpendicular orientations. The laser parameters used here are the same as those in Fig. 4 in Ref. [1]: the laser is linear polarization with a peak intensity of 6.5×10^{13} W/cm^2, a wavelength of 3100 nm and duration of 10 fs, which is shown in Fig. 3. For the parallel orientation (Fig. 4(a)), the electric field propagates along the molecular axis and the molecule gets its maximally distortion, which corresponds to a rapid elongation of C–H_1 bond, meanwhile, the C–H_2 bond decreases slowly and monotonously. The dynamics are different for the perpendicular orientation (Fig. 4(b)). We found that H_1 ion does not go as far as it in the parallel orientation (about 0.8 smaller). Meanwhile, C–H_2 bond first decreases and then increases in perpendicular case. Our TDDFT simulation results match well with the experiment results in Ref. [1].

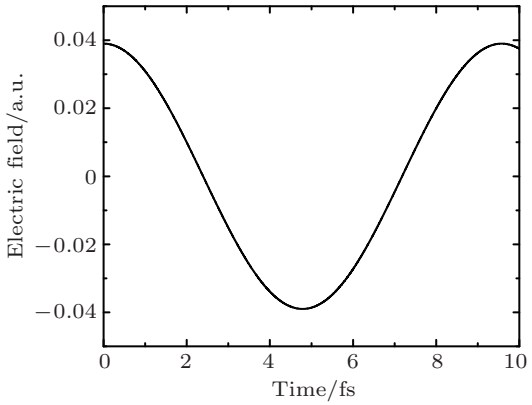

Fig. 3. The temporal profile of the electric field.

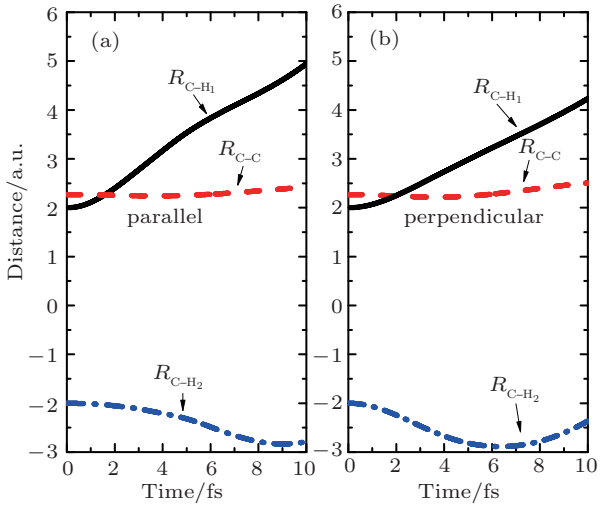

Fig. 4. Time evolution of chemical band C–H, C–C in (a) parallel and (b) perpendicular orientations.

Next, we will solve two questions: First, why the dynamics of C–H_1 bonds are different in parallel and perpendicular orientations? Second, why the dynamics of C–H_2 bonds are similar in parallel and perpendicular orientations?

To answer these questions, a classical force analysis is exhibited in Fig. 5. The force on an ion can be separated

to three parts as shown in Eq. (4): other ions, the electrons, and the laser field, respectively. Two features can be obtained from Fig. 5: First, the total force on the H_1 atom becomes smaller with the time evolves in parallel orientation, which causes the dynamic processes of H_1 are strongly determined by the force at the beginning time in this case; Meanwhile, for the perpendicular orientation, the total force on H_1 decreases to zero and then increases in the opposite direction at a similar magnitude. Second, We can see from this figure that before 5 fs, the total forces on both H_1 and H_2 have an oscillation in the parallel case and the oscillation is similar as the force from electrons. However, the perpendicular case does not have this phenomenon, the total forces in perpendicular case are smooth. This result indicates that the dynamics of H_1 and H_2 comes from the laser effect on the electrons, in other words, the alignment dependence of electron dynamics dominates the dissociation process.

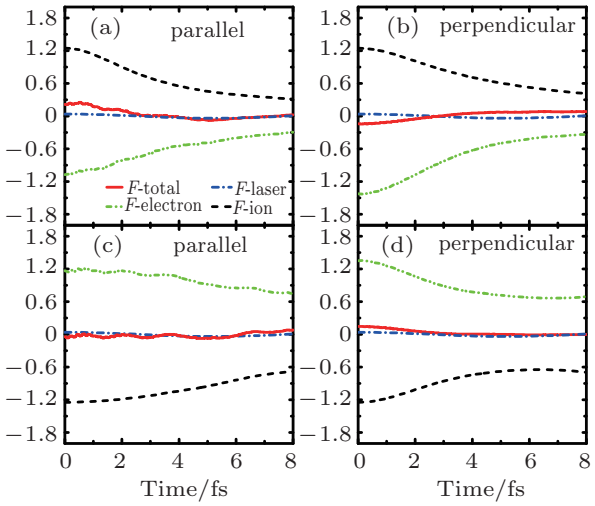

Fig. 5. Force analysis of H_1 [(a) and (b)] and H_2 [(c) and (d)] with parallel [(a) and (c)] and perpendicular orientations [(b) and (d)]. The red line, green dash dot–dot line, blue dash–dot–dash line, and black dash line are the total force, electron force, laser force, and ion force, respectively.

For explaining Fig. 5, we go back to Fig. 2 to analyze the initial density distribution of the $^3\Pi_u$ state. We can see from this figure that the density distribution is almost along the molecular axis, which indicate that the ionization yield should be larger at parallel case, this alignment dependence of the ionization yield is studied in many other works. For further supporting our results, we calculate the bond dynamics of H_2 with and without the laser pulse for the perpendicular case (the left panel of Fig. 6), and the ratio of the ionization yield between the parallel and perpendicular case (the right panel of Fig. 6). As we expected, the ionization yield from the parallel case is much bigger than that from the perpendicular case. In the perpendicular case, the H_2 atom dynamic from laser-free is almost the same as that from the with-laser one. This is because in the perpendicular case, the ionization by the laser is weak, therefore, the effect from laser on the electrons is neglectful, as a result, the dynamics from the perpendicular orientation is all most the same with the laser-free case.

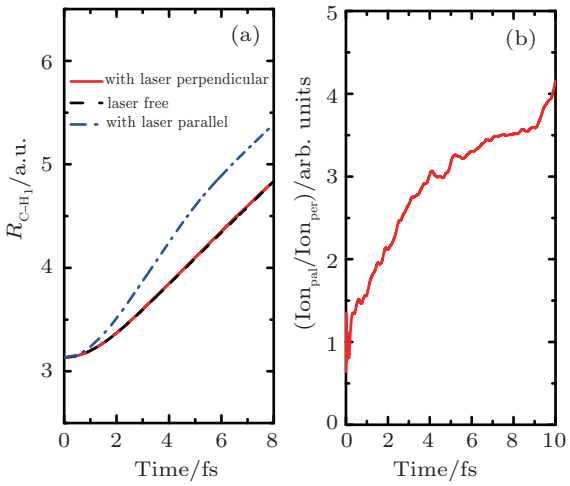

Fig. 6. (a) Time evolution of R_{CH_1} with parallel (blue dash line), perpendicular (red solid line), and the laser-free case (black dash line). (b) The ratio of the ionization yield between parallel and perpendicular orientations.

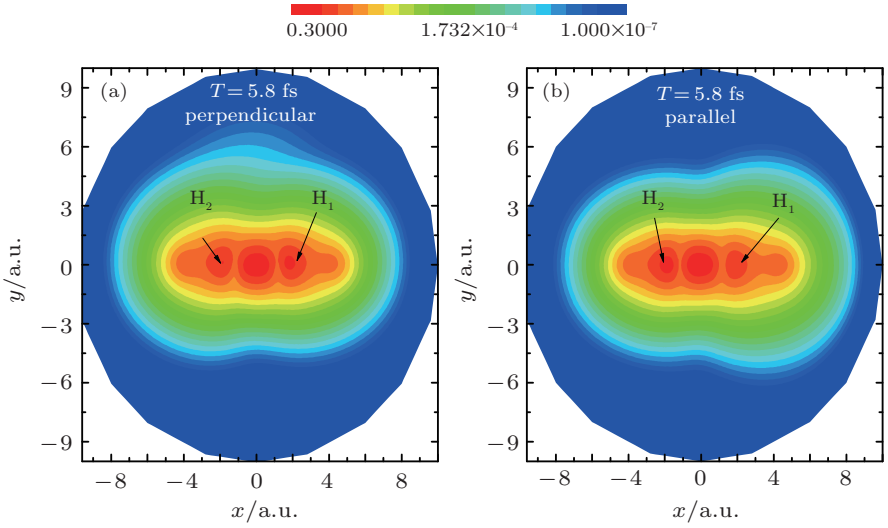

Fig. 7. Slice of the electron density distribution at $t = 5.8$ fs for (a) perpendicular and (b) parallel orientations.

Figure 7 shows the slice of the density distribution of $C_2H_2^{2+}$ at $t = 5.8$ fs. It can be noticed from Fig. 7 that, in the parallel case, the electron density of $C_2H_2^{2+}$ is asymmetrical, which makes the F_a^{e-i} is not equal to F_a^{i-i}. On the contrary, the density distribution from the perpendicular case is hardly changed. Thereby, the balance of F_a^{e-i} and F_a^{i-i} is not broken up. These results shows why H_2 in the perpendicular orientation does not elongate as rapid as that in the parallel case.

In order to investigate the alignment dependence of the photondissociation process from other linear molecules, we perform the TDDFT calculations on N_2 neutral molecule. The laser parameters are totally same as that in Fig. 5. The results are shown in Fig. 8: we can see from this figure N–N band in parallel case elongates faster than that in perpendicular case. This can be understood directly from our analysis above: in the parallel case, the ionization yield is larger, then the molecule becomes more unstable and dissociate quicker. From the calculations above, we can conclude that the alignment dependence of the photondissociation process is widespread in linear molecules.

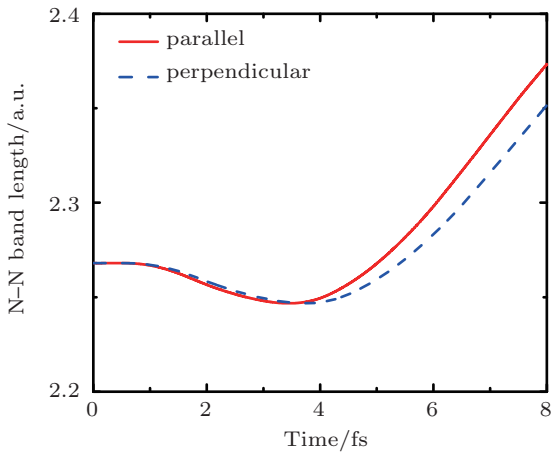

Fig. 8. Time evolution of N–N band length with parallel (red line) and perpendicular (blue dash line) orientations. The laser parameters are the same as those in Fig. 5.

4. Conclusion

In this work, we numerically investigated the proton dynamics of C_2H_2 testified in a strong laser field. Our TDDFT MD results show that the two C–H chemical bands in $C_2H_2^{2+}$ exhibit different dissociation behaviors with different orientation laser fields, which matches well with the experiment results. This results can be explained as the molecule in the parallel orientation has a larger ionization rate than in the perpendicular orientation, therefore, the forces from the electron on the proton are different, which leads to a different dissociation dynamics. We also perform a calculation on N_2 neutral molecule, an alignment dependence of the photondissociation process can be found as well, we can conclude that the alignment dependence of the photondissociation process is widespread in linear molecules. The calculations enables quantitative understanding of laser-induced ultrafast molecular dynamics at a electron-level.

References

[1] Wolter B, Pullen M G, Le A T, Baudisch M, Doblhoff-Dier K, Senftleben A, Hemmer M, Schröter C D, Ullrich J, Pfeifer T, Moshammer R, Gräfe S, Vendrell O, Lin C D and Biegert J 2016 *Science* **345** 308
[2] Ackermann W, et al. 2007 *Nat. Photon.* **1** 336
[3] Lopez C, Trimeche A, Comparat D and Picard Y J 2019 *Phys. Rev. Appl.* **11** 064049
[4] Hentschel M, Kienberger R, Spielmann C, Reider G A, Milosevic N, Brabec T, Corkum P, Heinzmann U, Drescher M and Krausz F 2001 *Nature* **414** 509
[5] Zhao Y T, Xu X Q, Jiang S C, Zhao X, Chen J G and Yang Y J 2020 *Phys. Rev. A* **101** 033413
[6] Zhao Y T, Jiang S C, Zhao X, Chen J G and Yang Y J 2020 *Opt. Lett.* **45** 2874
[7] Paul P M, Toma E S, Breger P, Mullot G, Augé F, Balcou P, Muller H G and Agostini P 2001 *Science* **292** 1689
[8] Martin J M, Bade S, Dubosclard W, Khan M A, Kim S, Garraway B M and Alzar C L G 2019 *Phys. Rev. Appl.* **12** 014033
[9] Hentschel M, Kienberger R, Spielmann C, Reider G A, Milosevic N, Brabec T, Corkum P, Heinzmann U, Drescher M and Krausz F 2001 *Nature* **414** 509
[10] Guan J, Behrendt V, Shen P, Hofsass S, Muthu-Arachchige T, Grzesiak J, Stienkemeier F and Dulitz K 2019 *Phys. Rev. Appl.* **11** 054073
[11] Drescher M, Hentschel M, Kienberger R, Uiberacker M, Yakovlev V, Scrinzi A, Westerwalbesloh T, Kleineberg U, Heinzmann U and Krausz F 2002 *Nature* **419** 803
[12] Schiffrin A, Paasch-Colberg T, Karpowicz N, Apalkov V, Gerster D, Muhlbrandt S, Korbman M, Reichert J, Schultze M, Holzner S, Barth J V, Kienberger R, Ernstorfer R, Yakovlev V S, Stockman M I and Krausz F 2013 *Nature* **493** 70
[13] Zhao Y, Ma S, Jiang S, Yang Y, Zhao X and Chen J 2019 *Opt. Express* **27** 34392
[14] Zhao X, Wei H, Wu Y and Lin C D 2017 *Phys. Rev. A* **95** 043407
[15] Zhao X, Wei H, Yu W W, Wang S J and Lin C D 2020 *Phys. Rev. Appl.* **13** 034043
[16] Griesser H P, Perrella C, Light P S and Luiten A N 2019 *Phys. Rev. Appl.* **11** 054026
[17] Luo Y and Zhang P 2019 *Phys. Rev. Appl.* **12** 044056
[18] Haruyama J, Hu C and Watanabe K 2012 *Phys. Rev. A* **85** 062511
[19] Russakoff A and Varga K 2015 *Phys. Rev. A* **92** 053413
[20] Telnov D A and Chu S I 2009 *Phys. Rev. A* **80** 043412
[21] Le Breton G, Rubio A and Tancogne-Dejean N 2018 *Phys. Rev. B* **98** 165308
[22] Tully J C and Preston R K 1971 *J. Chem. Phys.* **55** 562
[23] Meyer H D, Manthe U and Cederbaum L S 1990 *Chem. Phys. Lett.* **165** 73
[24] Xue S, Du H, Hu B, Lin C D and Le A T 2018 *Phys. Rev. A* **97** 043409
[25] Andrade X, Alberdi-Rodriguez J, Strubbe D A, Oliveira M J T, Nogueira F, Castro A, Muguerza J, Arruabarrena A, Louie S G and Aspuru-Guzik A 2012 *J. Phys.: Condens. Matter* **24** 233202
[26] Casto A, Appel H, Oliveira M, Rozzi C A, Andrade X, Lorenzen F, Marques M A L, Gross E K U and Rubio A 2006 *Phys. Status Solidi B* **243** 2465
[27] Marques M A L, Castro A, Bertsha G F and Rubio A 2003 *Comput. Phys. Commun.* **151** 60
[28] Troullier N and Martins J L 1991 *Phys. Rev. B* **43** 1993
[29] Perdew J P and Zunger A 1981 *Phys. Rev. B* **23** 5048
[30] Doblhoff-Dier K, Kitzler M and Gräfe S 2016 *Phys. Rev. A* **94** 013405